www.sciencemag.org/cgi/content/full/science.aac4255/DC1

Supplementary Materials for

Commensal *Bifidobacterium* promotes antitumor immunity and facilitates anti–PD-L1 efficacy

Ayelet Sivan, Leticia Corrales, Nathaniel Hubert, Jason B. Williams, Keston Aquino-Michaels, Zachary M. Earley, Franco W. Benyamin, Yuk Man Lei, Bana Jabri, Maria-Luisa Alegre, Eugene B. Chang, Thomas F. Gajewski*

*Corresponding author. E-mail: tgajewsk@medicine.bsd.uchicago.edu

Published 5 November 2015 on *Science* Express
DOI: 10.1126/science.aac4255

This PDF file includes

Other Supplementary Material for this manuscript includes the following:
(available at www.sciencemag.org/cgi/content/full/science.aac4255/DC1)

Materials and Methods

Animals and tumor model

C57BL/6 mice were obtained from Jackson laboratory or Taconic farms. For all experiments 6–8-week-old female mice were used. Mice were fed Harlan Teklan 2018 diet and housed in the SPF University of Chicago animal facility. The C57BL/6-derived melanoma cell line B16.F10.SIY (henceforth referred to as B16.SIY) was generated as described (*33*). The MB49 bladder cancer cell line was originally a generous gift from Timothy L. Ratliff, Purdue University. For tumor growth experiments, mice were injected subcutaneously with 1×10^6 B16.SIY tumor cells or parental B16.F10 tumor cells. For bladder cancer model experiments, mice were injected subcutaneously with $2x10^6$ MB49 cells. Tumor size was measured twice a week until endpoint and tumor volume was determined as length $\times$ width$^2 \times 0.5$. All experimental animal procedures were approved by the University of Chicago Animal Care and Use Committee (IACUC).

IFN-γ ELISPOT and SIY Pentamer analyses

ELISPOT plates (*Millipore, MAIP S4510*) were coated with purified αIFN-γ (*BD*) overnight at 4 degrees. Plates were blocked with 10% FBS in DMEM for 2 hours at room temperature. Whole splenocytes were plated at 10^6 cells per well and stimulated with SIY peptide overnight at 37^{o}C. Spots were developed using the BD mouse IFN-γ kit (*Cat. No. 552569*), and the number of spots was measured using an Immunospot Series 3 Analyzer and analyzed using ImmunoSpot software (Cellular Technology). For pentamer staining, cells were labeled with PE-MHC class I pentamer (*Proimmune*) consisting of murine H-2K^b complexed to SIYRYYGL (SIY) peptide or to control SIINFEKL peptide, and stained with CD3-AX700 (*Ebioscience, 17A2*), CD8-PacBlue (*Biolegend, 53-6.7*), CD4-APC (*Pharmingen, RM4-5*), CD62L-PECy7 (*Ebioscience, MEL-14*), CD44-FITC (*BD, IM7*) and Fixable Viability-ef780 (*Ebioscience*). Stained cells were analyzed using an LSR II cytometer with FACSDiva software (BD). Data analysis was conducted with FlowJo software (Tree Star).

Fecal transfers and αPD-L1 mAb immunotherapy

Fecal pellets from JAX and TAC-derived mice were collected upon arrival in our facility and each fecal pellet was resuspended in 1 ml of phosphate-buffered saline (PBS). The suspension from each fecal pellet was used for oral gavage of two recipient mice, 100µl per gavage. For prophylactic fecal transfer experiments mice were gavaged with JAX or TAC fecal suspensions once a week for two weeks prior to tumor inoculation. For therapeutic fecal transfer experiments, mice were gavaged on days 7 and 14 post tumor implantation. For combination therapy experiments, mice were additionally injected intraperitoneally with 100µg αPD-L1 mAb (clone 10f.9g2, *BioXCell*) in 100µl PBS on days 7, 10, 13 and 16 post-tumor implantation.

Microbial DNA analysis

Bacterial DNA was extracted from murine fecal pellets using PowerSoil®-htp 96 Well Soil DNA Isolation Kit (MoBio cat.# 12955-4). The V4-V5 region of the 16S rRNA encoding gene was amplified (http://www.earthmicrobiome.org/emp-standard-protocols/; Earth Microbiome Project, 2011) and sequenced at the High-Throughput Genome

Analysis Core at Argonne National Laboratory. Quantitative Insights Into Microbial Ecology (QIIME) was used to trim and classify sequences (*34*); specifically, the open reference OTU picking protocol was used at 97% sequence identity against the Greengenes database (05/13 release) (*35*). PYNAST was used to align sequences (*36*) and RDP Classifier was used for taxonomic assignment (*37*). Community structure was compared using weighted and unweighted UniFrac distances (*38*). All beta-diversity analyses were performed on data rarefied to 9662 reads and after filtering out OTUs occurring in less than 35% of samples per comparison. Non-parametric t-tests were performed to determine differences in bacterial taxa occurrence between fecal communities. Principal Coordinate Analysis (PCoA) ordination was generated to visually compare beta diversity and Analysis of Similarity (ANOSIM) test statistics were performed to statistically compare within- to between- group similarity in QIIME. Newick tree files comprised of OTUs deemed significant by t-test were constructed in iTOL (*39*); bar graphs representing mean log fold differences in relative abundances were plotted for each taxon alongside the phylogeny, replacing zero values with the least non-zero value observed in the comparison.

Association testing was performed via standard linear regression. We tested the association between frequency of SIY^+CD8^+ T cells in the tumor and taxa relative abundance. We used rarefied values and removed taxa that were missing in greater than 35% of the samples. The first two principal components of the relative abundance matrix were used as covariates in the model. Specifically we fit

$$SIY \sim relative\_abundance_k + PC1 + PC2$$

where k is the kth taxa. The association was fit with *lm*, principal components were calculated using the package *PEER* and FDR was computed using the package *qvalue*. This analysis was performed in R.

OTU_681370 was characterized via NCBI Microbial Genomes Blast, using the V4-V5 16s rRNA sequence:
TACGTAGGGTGCAAGCGTTATCCGGATTTATTGGGCGTAAAGGGCTCGTAGG
CGGTTCGTCGCGTCCGGTGTGAAAGTCCATCGCTTAACGGTGGATCCGCGCC
GGGTACGGGCGGGCTTGAGTGCGGTAGGGGAGACTGGAATTCCCGGT.

Bacterial administration and heat inactivation

A cocktail of lyophilized *Bifidobacterium* species (*B. bifidum, B. longum, B. lactis and B. breve*, Seeking Health) was resuspended in PBS at $5x10^9$ CFU/ml. Each mouse was given 200µl of *Bifidobacterium* ($1x10^9$ CFU/mouse) by oral gavage 7 and 14 days following tumor inoculation. Heat inactivation was performed by boiling rehydrated bifidobacteria at 100°C for 2 hours. Heat-treated and live bifidobacteria were serially diluted in reduced PBS and plated on reduced clostridial medium (RCM) agar in anaerobic conditions. Plates were subsequently incubated in an anaerobic chamber for three days to test efficacy of killing. For gavage of ATCC-derived bifidobacterial cultures, ATCC 15700 *B. breve* and ATCC BAA-999 *B. longum* were cultured in RCM in an anaerobic chamber and monitored for log-phase growth using spectrophotometric measurements of turbidity every hour. At measurements of ~0.5, cultures were pelleted, resuspended at $5x10^9$ cells/ml PBS (as assessed by serial dilution and quantification of colony forming units, following plating on RCM agar plates and incubation in an anaerobic chamber for 48 hours) and gavaged into mice, 200ul/mouse, $1x10^9$

cells/mouse. *Lactobacillus murinus* (provided by Yuan Zhang and Yang-Xin Fu at University of Chicago) was cultured in MRS broth overnight, then washed and resuspended in PBS at $5x10^{10}$ CFU/ml. Each mouse was orally gavaged with 100µl of bacterial suspension ($5x10^9$ CFU/mouse) 7 and 14 days following tumor inoculation.

CD8$^+$ T Cell Depletion

For depletion of CD8$^+$ T cells, mice were injected intraperitoneally weekly with rat mAb anti-mouse CD8 (43.2) or isotype control IgG2b (BioXcell) at a dose of 250 µg per mouse. These regimens resulted in > 99% depletion of CD8$^+$ T cells from the peripheral blood, as evaluated by flow cytometry.

Bacterial quantitation in peripheral organs and fecal samples

Mesenteric lymph nodes, tumor and spleen were sterilely removed, homogenized in PBS and strained through a 70µm filter. The cells were pelleted, resuspended in QIAGEN buffer ALT, and underwent Qiashredding (QIAGEN) to further lyse cells and reduce the viscosity. DNA was purified from the flow through using QIAGEN DNA mini purification kit. For spiking experiments, organs were isolated as described above and spiked with 10^9, 10^6, 10^3, 10^2 and 10 ATCC 15700 *B. breve* cells, as assessed by serial dilution of anaerobically cultured bacteria, incubating 48 hours on RCM agar plates in anaerobic conditions, and counting colony forming units. Real time quantitative PCR (qPCR) was used to quantify bacterial SSU (16S) rRNA gene abundance, in the feces and tissue as described previously (*40-42*). Primer sets targeting SSU rRNA genes of bifidobacteria at the genus level were used and included BifidF (CGG GTG AGT AAT GCG TGA CC), and BifidR (TGA TAG GAC GCG ACC CCA) and probe (6FAM-CTC CTG GAA ACG GGT G) (*42*). Primers and probe were synthesized by IDT and Invitrogen respectively. qPCR master mixes contained TaqMan Universal qPCR 1X Master Mix (Applied-Biosystems), 0.25µM primers and probe, and either 4ng (feces) or 25ng (tissue) gDNA template. Purified genomic DNA from reference bacteria *Bifidobacterium breve* ATCC 15700D-5 was used as a standard. Cycling conditions were 50°C for 2min, 95°C for 10min, and 45 cycles of 95°C for 15sec, 60°C for 60sec using Roche Lightcycler 480 real time PCR machine. A melt curve was performed for quality assurance and efficiencies ranged under the accepted values, 90-110%. Data were normalized as copies of bacterial 16S per ng DNA.

CFSE-labeled 2C CD8$^+$ T cell adoptive transfer

CD8$^+$ T cells were isolated from the spleen and lymph node of naïve CD45.1/.2$^+$ 2C TCR Tg mice using the MACS CD8 T cell Isolation Kit (*Miltenyi, Cat No. 130-095-236*), labeled with 2.5 mM CFSE and injected i.v. into CD45.2$^+$ C57BL/6 mice derived from either JAX or TAC and into TAC mice gavaged with *Bifidobacterium* once a week for two weeks. 24 hours later, mice were inoculated with $1x10^6$ B16.SIY melanoma cells s.c. Seven days post-adoptive T cell transfer, spleen and tumor-draining lymph node were harvested and restimulated ex-vivo with SIY peptide in the presence of brefeldin A. Samples were stained with Fixable Viability-ef780 (*Ebioscience*), CD45.1-PerCPCy5.5 (*Ebioscience, E20*), CD45.2-APC (*Ebioscience, 104*), CD3-AX700 (*Ebioscience, 17A2*), CD8-BV711 (*Biolegend, 53-6.7*), CD4-BV605 (*Biolegend, RM4-5*) and IFN-γ-PE (*BD,*

XMG1.2). Intracellular IFN-γ production and CFSE dilution were assessed in gated CD45.1/.2$^+$ 2C CD8$^+$ T cells by flow cytometry.

Dendritic cell sorting and gene expression profiling

Upon arrival in our facility, TAC mice were gavaged with *Bifidobacterium* once a week for two weeks. *Bifidobacterium*-fed mice, newly arrived JAX mice, and newly arrived TAC mice were inoculated subcutaneously in both flanks with 5x10^6 DRAQ5-labeled B16.SIY tumor cells. 40hrs following tumor implantation, whole tumors including infiltrating immune cells were digested in collagenase (*Worthington*) and filtered into single cell suspensions. Samples from 5 mice in each group were pooled and subsequently stained with Fixable Viability-ef506 (*Ebioscience*), CD45-AF488 (*Bioloegend, 30-F11*), CD3-ef450 (*Ebioscience, 145-2C11*), CD19-PB (*Ebioscience, 1D3*), I-A/I-E-PECy7 (*Biolegend, M5/114.15.2*), CD11c-PE (*Ebioscience, N418*) and CD11b-PerCpCy5.5 (*BD, M1/70*). Live CD45$^+$CD3$^-$CD19$^-$MHCII^{hi}CD11c$^+$ dendritic cells were sorted directly into RLT Buffer (*Qiagen*) using FACSAriaIII (*BD*) and stored immediately on dry ice. Total RNA was isolated using RNeasy® Micro kit (*Qiagen*). RNA was submitted to the Functional Genomics Facility at the University of Chicago for gene expression profiling. RNA integrity and concentration were assessed using an Agilent Bioanalyzer 2100, and all RNA samples used for microarray analysis had an RNA Integrity Number > 9.0. Total RNA was processed into biotinylated cRNA using the Epicentre TargetAmp™ 2-Round Biotin-aRNA Amplification Kit 3.0 (*TAB2R71024*). The cRNA was hybridized to Illumina MouseRef8v2 arrays using Illumina provided protocols and scanned using an Illumina HiScan. Quantile normalized and background subtracted values were subsequently analyzed using R. Genes whose expression value was under 10 were removed from the analysis. Mean fold-change in gene transcript levels between JAX samples relative to TAC, and BIF samples relative to TAC were calculated, and genes whose fold-change was over 1.5 in both comparisons (760 gene transcripts) were inputted into *The **D**atabase for **A**nnotation, **V**isualization and **I**ntegrated **D**iscovery (**DAVID**)* v6.7 for pathway analysis. Genes found to be significantly enriched ($p<0.05$) for immune function were then plotted in a heatmap using R software.

Quantitative PCR validation of gene-expression profiling

DCs were sorted and RNA extracted as described above. cDNA was synthesized using High Capacity cDNA Reverse Transcription Kit (Applied Biosystems). Gene expression was measured by real-time qRT-PCR using specific primers/probes (Roche Universal Probe library, **Table S7**). PCR was performed using 7300 Real Time PCR machine (Applied Biosystems). The results are expressed as fold-change over TAC, normalized to 18S expression.

BMDC stimulation with *Bifidobacterium* in vitro

Cells isolated from the tibiae and femurs of WT C57BL/6 mice were cultured in DMEM medium containing 10% FBS and 1% penicillin/streptomycin, in the presence of rmGM-CSF (20 ng/ml; BioLegend) for 8 days at 37°C with 5% CO2. BMDCs were then stimulated for 4 hours with medium alone or with rehydrated *Bifidobacterium*-containing medium at a ratio of 1:10 BMDCs to bacterial cells. Total RNA was isolated using

RNeasy® Micro kit (*Qiagen*) and submitted to the Functional Genomics Facility at the University of Chicago for gene expression profiling. RNA integrity and concentration were assessed using an AgilentBioanalyzer 2100, and all RNA samples used for microarray analysis had an RNA Integrity Number = 10.0.

Dendritic cell stimulation of CFSE-labeled 2C $CD8^+$ T cells in vitro

Upon arrival in our facility, TAC mice were gavaged with *Bifidobacterium* once a week for two weeks. DCs were purified from peripheral lymphoid tissues of $CD45.2^+$ C57BL/6 naive *Bifidobacterium*-fed mice, newly arrived JAX mice, and newly arrived TAC using Pan Dendritic cell Isolation Kit (*Miltenyi, Cat No.* 130-100-875). $2x10^5$ DCs were plated 1:1 with $CD45.1/.2^+$ CFSE- labeled 2C $CD8^+$ T cells (MACS $CD8^+$ T cell Isolation Kit (*Miltenyi, Cat No. 130-095- 236*) and incubated at 37°C for 72 hours in the presence of varying concentrations of SIY peptide. Brefeldin A was added for 6 additional hours. Samples were stained with Fixable Viability-ef780 (*Ebioscience*), CD45.1-PerCPCy5.5 (*Ebioscience, E20*), CD45.2-APC (*Ebioscience, 104*), CD3-AX700 (*Ebioscience, 17A2*), CD8-BV711 (*Biolegend, 53-6.7*), CD4-BV605 (*Biolegend, RM4-5*) and IFN-γ-PE (*BD, XMG1.2*). Intracellular IFN-γ production and CFSE dilution were assessed in gated CD45.1/.2+ 2C $CD8^+$ T cells by flow cytometry.

Statistical analysis

Tumor growth curves were analyzed using two-way ANOVA, with either Sidak's multiple comparisons post test for comparison of two groups, Dunnett's multiple comparisons post test for comparison between multiple groups and a control group, or Tukey's multiple comparisons post test for comparison of more than two groups to each other. For other comparisons, unpaired Student's *t*-test was used when comparing two groups and one-way ANOVA with Holm Sidak correction for multiple testing was used when comparing more than two groups. Microbial composition comparisons were performed using non-parametric *t*-tests. If samples were not independent (technical replicates of pooled samples), linear mixed model regression was used with Bonferroni correction for multiple testing. $P<0.05$ was considered statistically significant and denoted as follows: $^*P < 0.05$, $^{**}P < 0.01$, $^{***}P < 0.001$, $^{****}P < 0.0001$. Statistical analysis was performed using GraphPad PRISM and R.

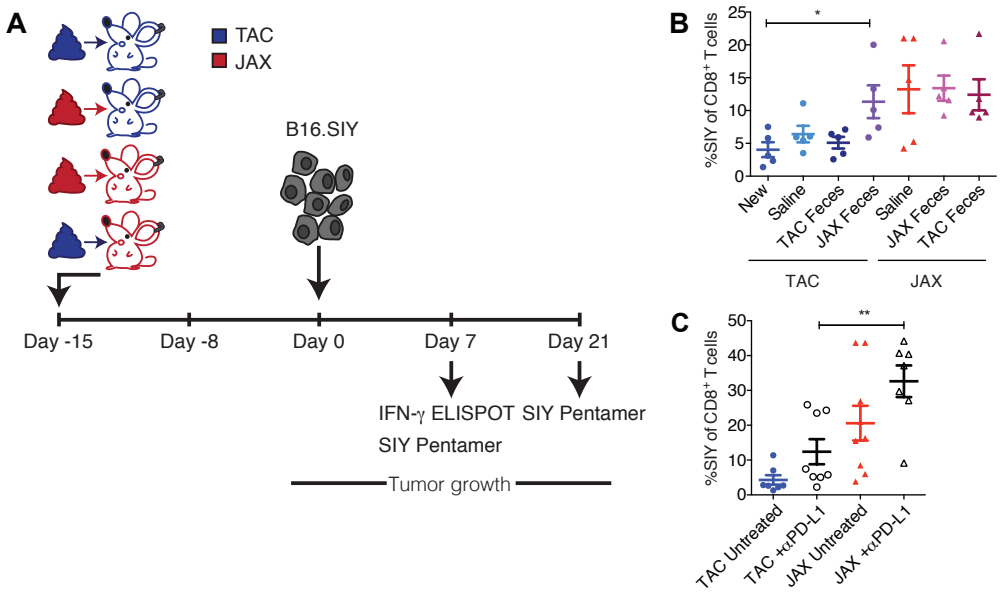

Fig. S1.

(A) Schematic of prophylactic fecal transfer. Fecal pellets collected from JAX and TAC mice upon arrival in our facility were resuspended in PBS, homogenized and the supernatant was introduced by oral gavage into either JAX or TAC recipients as shown, once a week for two weeks prior to B16.SIY tumor inoculation. **(B)** Percentage of SIY^+ T cells of total $CD8^+$ T cells within the tumor of groups as in Figure 2A, determined by flow cytometry 7 days post-tumor inoculation. **(C)** Percentage of SIY^+ T cells of total $CD8^+$ T cells within the tumor of JAX and TAC mice, untreated or treated with αPD-L1 mAb, as determined by flow cytometry 21 days post-tumor inoculation. Data show individual mice with mean +/- SEM analyzed by one-way ANOVA with Holm-Sidak correction for multiple comparisons; data are representative (B) or combined (C) from at least two independent experiments; 5 mice per group per experiment; $^*P < 0.05$, $^{**}P < 0.01$.

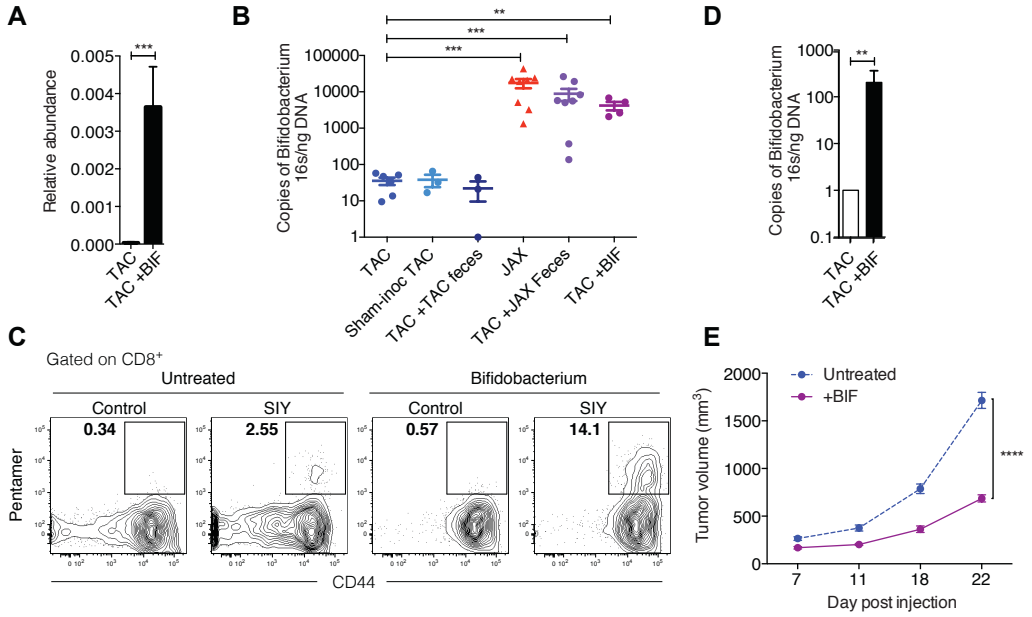

Fig. S2

(A) Relative abundance of *Bifidobacterium* OTU_681370 in fecal material obtained from TAC mice 7 days following inoculation with commercial *Bifidobacterium* species. **(B)** *Bifidobacterium* levels in fecal material obtained from groups as shown, assessed by qPCR using genus-specific primers. **(C)** Representative plots showing percentage of SIY^+ T cells of total $CD8^+$ T cells within the tumor of untreated and *Bifidobacterium*-treated TAC mice, as assessed by flow cytometry 14 days following start of treatment. **(D)** *Bifidobacterium* levels in TAC mice 3 weeks post *Bifidobacterium* administration, assessed by qPCR**. (E)** B16.SIY tumor growth in TAC mice, untreated or inoculated with *Bifidobacterium* 6 weeks prior to tumor implantation. Data show mean +/- SD (A) or SEM [(D), (E)], or individual mice with mean +/- SEM (B), analyzed by non parametric *t*-tests [(A), (B), (D)] or two-way ANOVA with Sidak's correction (E); $n = 5\text{-}10$ mice per group; $^{**}P < 0.01$, $^{***}P < 0.001$, $^{****}P < 0.0001$.

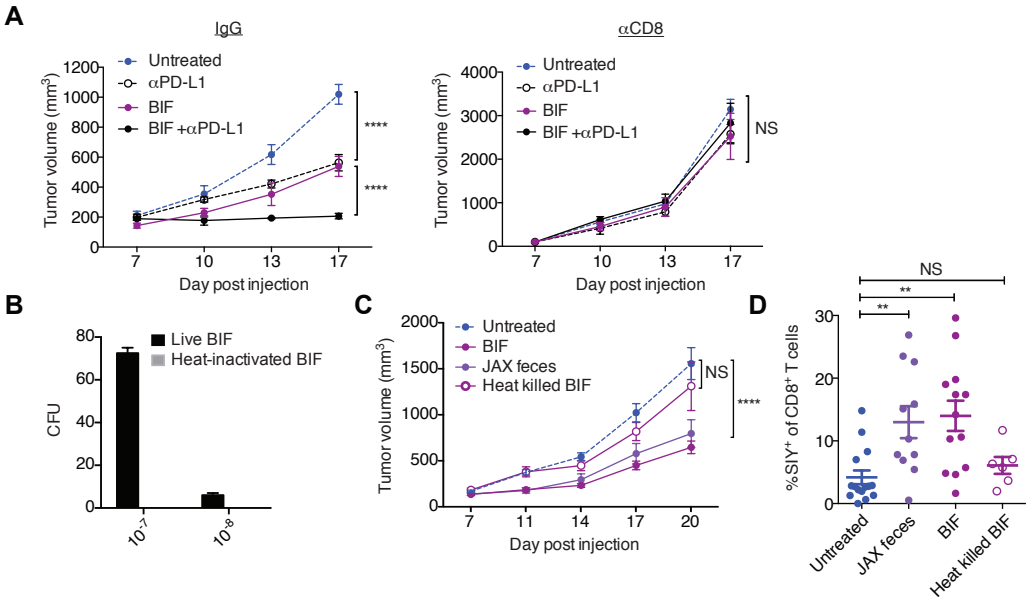

Fig. S3

A) B16.SIY tumor growth for isotype-treated (left) or CD8-depleted (right) groups as in Figure 3E**. (B)** Number of colony forming units (CFU) of live and heat inactivated bifidobacteria, plated in RCM agar following serial dilution in reduced PBS and incubated in an anaerobic chamber for 72 hours. Bars represent 2 replicate plates of each dilution. **(C)** B16.SIY tumor growth kinetics in TAC mice, untreated or treated with live *Bifidobacterium*, heat inactivated *Bifidobacterium* or JAX fecal material 7 and 14 days post tumor implantation. **(D)** Percentage of tumor-infiltrating SIY^+ T cells of total $CD8^+$ T cells for treatment groups as in (C), determined by flow cytometry 14 days after start of treatment. Data show mean +/- SEM analyzed by two-way ANOVA with Tukey's (A) or Dunnett's (C) correction for multiple comparisons; or individual mice with mean +/- SEM analyzed by one-way ANOVA with Holm-Sidak correction for multiple comparisons (D); data are representative [(A) and (B)] or combined [(C) and (D)] from at least two independent experiments; 5 mice per group per experiment; $^{**}P < 0.01$, $^{****}P < 0.0001$, NS, not significant.

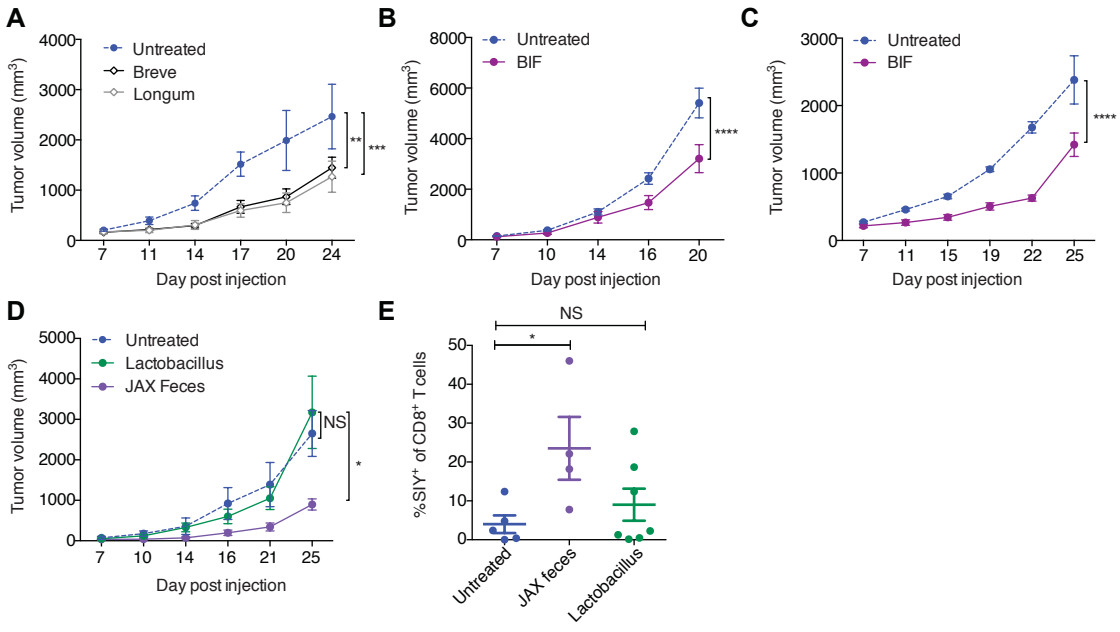

Fig. S4

(A) B16.SIY tumor growth kinetics in TAC mice, untreated or treated with ATCC-derived *B. breve* or *B. longum*. **(B)** B16.F10 tumor growth kinetics in TAC mice, untreated or treated with *Bifidobacterium* 7 and 14 days post tumor implantation. **(C)** MB49 tumor growth kinetics in TAC mice, untreated or treated with *Bifidobacterium* 7 and 14 days post tumor implantation. **(D)** B16.SIY tumor growth kinetics in TAC mice, untreated or treated with *Lactobacillus murinus* or JAX fecal material 7 and 14 days post tumor implantation. **(E)** Percentage of tumor-infiltrating SIY^+ T cells of total $CD8^+$ T cells for treatment groups as in (D), determined by flow cytometry 18 days after start of treatment. Data show mean +/- SEM [(A) - (D)] or individual mice with mean +/- SEM (E), analyzed by two-way ANOVA with Dunnett's [(A), (D)] or Sidak's correction [(B), (C)], or one-way ANOVA with Holm-Sidak correction for multiple comparisons (E); *n = 5-10* mice per group; $^{*}P < 0.05$, $^{**}P < 0.01$, $^{***}P < 0.001$, $^{****}P < 0.0001$, NS, not significant.

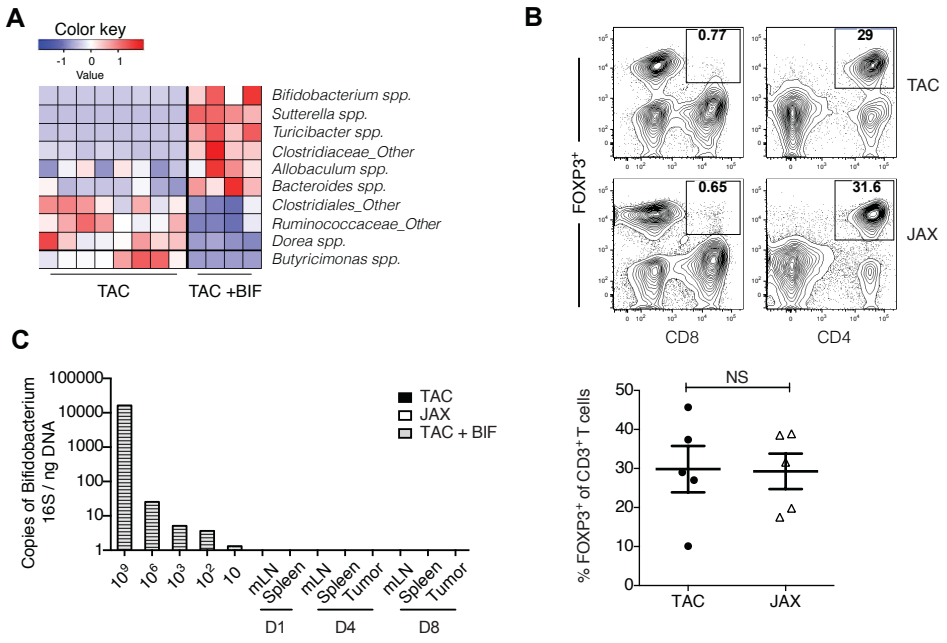

Fig. S5

(A) Heatmap demonstrating relative abundance of significantly altered genus-level taxa in *Bifidobacterium*-fed TAC mice FDR<0.05 (non-parametric *t*-test); columns depict individual mice; *n = 4-8* mice per group. **(B)** Frequency of $CD4^+$ $FOXP3^+$ T cells in tumors isolated from JAX and TAC mice 21 days post tumor inoculation, assessed by flow cytometry; representative plot (**top**), quantification (**bottom**). Data show individual mice with mean +/- SEM, analyzed by student's *t*-test; *n = 5* mice per group; NS, not significant. **(C)** Evaluation of translocation of *Bifidobacterium* into mesenteric lymph nodes (mLN), spleen and tumor of TAC, JAX and *Bifidobacterium*-inoculated mice, assessed by qPCR. Data show 5 mice per group over 3 time points.

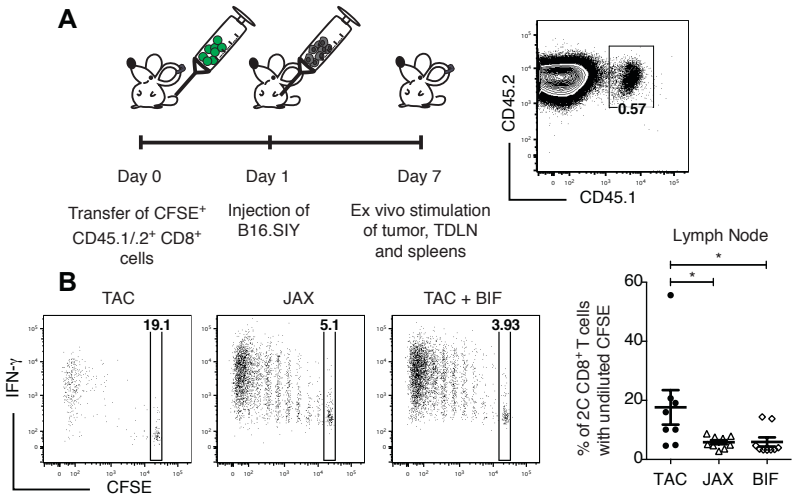

Fig. S6

(A) Schematic of *in vivo* 2C proliferation assays. $CD8^+$ T cells were isolated from the spleen and lymph node of naïve 2C TCR Tg $CD45.1^+/.2^+$mice, labeled with CFSE and injected i.v. into $CD45.2^+$ C57BL/6 mice derived from either TAC, JAX or *Bifidobacterium*-treated TAC mice. 24 hours later, mice were inoculated with $1x10^6$ B16.SIY melanoma cells s.c. Spleen and tumor-draining lymph node were harvested and restimulated ex-vivo with SIY peptide. Intracellular IFN-γ production and CFSE dilution were assessed in gated $CD45.1^+/.2^+$ 2C T cells by flow cytometry; TDLN=tumor-draining lymph node. **(B)** Representative CFSE dilution assessed in gated $CD45.1^+/.2^+$ 2C T cells by flow cytometry (**left**) and quantification (**right**). Data show individual mice +/- SEM and are representative of two independent experiments, 8 mice per group per experiment; analyzed by one-way ANOVA with Holm-Sidak correction; $^*P < 0.05$.

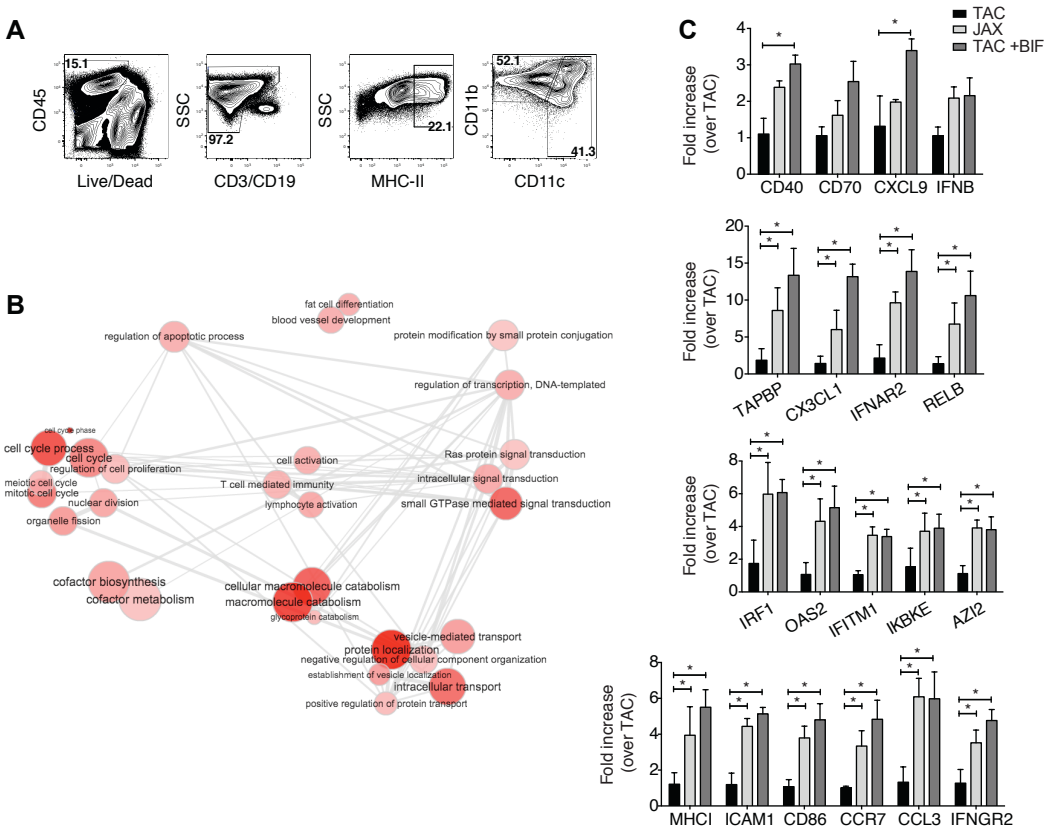

Fig. S7

(A) Representative plots depicting the strategy for isolation of DCs from tumors in JAX, TAC and *Bifidobacterium*-treated TAC mice: live $CD45^{+}CD3^{-}CD19^{-}MHCII^{hi}CD11c^{+}$ dendritic cells were sorted as shown. **(B)** All enriched biological pathways and functions found within the subset of elevated genes (fold change ≥ 1.5) in JAX and *Bifidobacterium*-treated TAC-derived DCs relative to untreated TAC DCs isolated from tumors 40hrs post inoculation, as assessed by DAVID pathway analysis. **(C)** qPCR validation of genes identified by microarray gene expression profiling as in (B). Data show mean +/-SEM, and are combined from two to three independent experiments, 5 mice pooled per sample, per experiment; analyzed by student's *t*-test **FDR<0.5*.

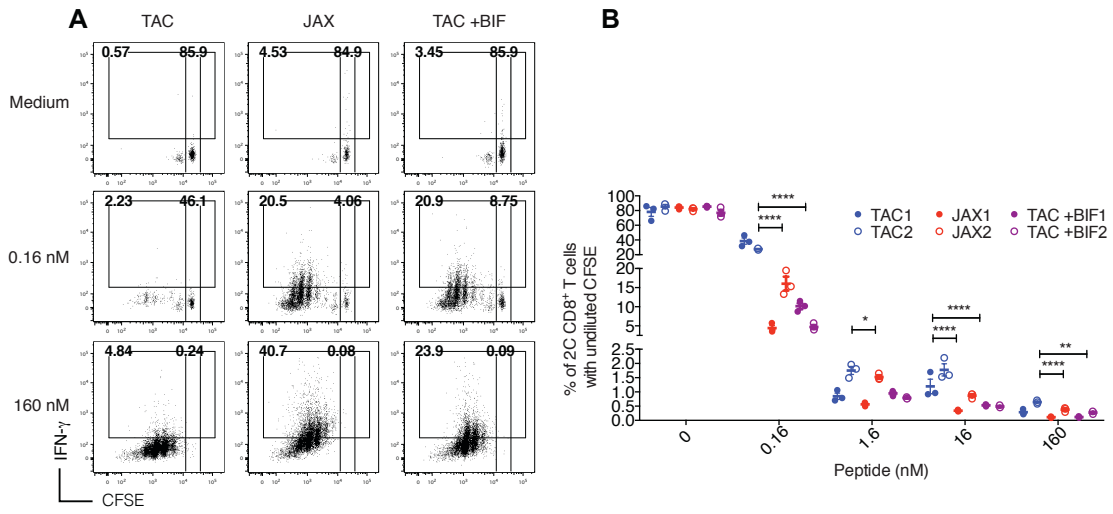

Fig. S8

(A) Representative flow plots of CFSE dilution and IFN-γ production in 2C $CD8^+$ T cells stimulated in vitro with DCs purified from naive TAC, JAX and *Bifidobacterium*-treated TAC mice in the presence of different concentrations of SIY peptide as shown. **(B)** Percentage of 2C $CD8^+$ T cells with undiluted CFSE, stimulated in vitro with DCs purified from naive TAC, JAX and *Bifidobacterium*-treated TAC mice in the presence of different concentrations of SIY peptide as shown. Data are combined from two independent experiments**,** 5 mice pooled per group per experiment, and show technical replicates of pooled samples from each experiment separately; analyzed by fitting a linear mixed model, with Bonferroni correction for multiple comparisons; $^{*}P < 0.05$, $^{**}P < 0.01$, $^{****}P < 0.0001$.

Table S1. Comparison of bacterial abundance between JAX and TAC mice, sham-, TAC-, and JAX-fed TAC mice at sequence level.

Table S2. Comparison of bacterial abundance between JAX and TAC mice, sham-, TAC-, and JAX-fed TAC mice at genus level.

Table S3. Univariate association testing between bacterial abundance and antigen-specific T cell infiltration across all permutation groups at sequence and genus levels.

Table S4. Comparison of bacterial abundance between TAC and *Bifidobacterium*-fed TAC mice at sequence and genus levels.

Table S5. Gene expression profiling results (Illumina microarray) comparing gene expression in DCs isolated from tumors of TAC, JAX, and *Bifidobacterium*-fed TAC mice.

Table S6. Gene expression profiling results (Illumina microarray) comparing gene expression in BM-DCs untreated or stimulated with *Bifidobacterium* in vitro.

Table S7. Primer sequences and probes (Roche Universal Probe Library) for qPCR validation of gene transcripts up-regulated by ≥1.5-fold in both JAX and *Bifidobacterium*-treated TAC-derived DCs relative to DCs from untreated TAC mice.

REFERENCES

1. F. S. Hodi, S. J. O'Day, D. F. McDermott, R. W. Weber, J. A. Sosman, J. B. Haanen, R. Gonzalez, C. Robert, D. Schadendorf, J. C. Hassel, W. Akerley, A. J. van den Eertwegh, J. Lutzky, P. Lorigan, J. M. Vaubel, G. P. Linette, D. Hogg, C. H. Ottensmeier, C. Lebbé, C. Peschel, I. Quirt, J. I. Clark, J. D. Wolchok, J. S. Weber, J. Tian, M. J. Yellin, G. M. Nichol, A. Hoos, W. J. Urba, Improved survival with ipilimumab in patients with metastatic melanoma. *N. Engl. J. Med.* **363**, 711–723 (2010). Medline doi:10.1056/NEJMoa1003466

2. O. Hamid, C. Robert, A. Daud, F. S. Hodi, W. J. Hwu, R. Kefford, J. D. Wolchok, P. Hersey, R. W. Joseph, J. S. Weber, R. Dronca, T. C. Gangadhar, A. Patnaik, H. Zarour, A. M. Joshua, K. Gergich, J. Elassaiss-Schaap, A. Algazi, C. Mateus, P. Boasberg, P. C. Tumeh, B. Chmielowski, S. W. Ebbinghaus, X. N. Li, S. P. Kang, A. Ribas, Safety and tumor responses with lambrolizumab (anti-PD-1) in melanoma. *N. Engl. J. Med.* **369**, 134–144 (2013). Medline doi:10.1056/NEJMoa1305133

3. P. C. Tumeh, C. L. Harview, J. H. Yearley, I. P. Shintaku, E. J. Taylor, L. Robert, B. Chmielowski, M. Spasic, G. Henry, V. Ciobanu, A. N. West, M. Carmona, C. Kivork, E. Seja, G. Cherry, A. J. Gutierrez, T. R. Grogan, C. Mateus, G. Tomasic, J. A. Glaspy, R. O. Emerson, H. Robins, R. H. Pierce, D. A. Elashoff, C. Robert, A. Ribas, PD-1 blockade induces responses by inhibiting adaptive immune resistance. *Nature* **515**, 568–571 (2014). Medline doi:10.1038/nature13954

4. S. Spranger, R. M. Spaapen, Y. Zha, J. Williams, Y. Meng, T. T. Ha, T. F. Gajewski, Up-regulation of PD-L1, IDO, and T(regs) in the melanoma tumor microenvironment is driven by CD8(+) T cells. *Sci. Transl. Med.* **5**, 200ra116 (2013). Medline doi:10.1126/scitranslmed.3006504

5. R. R. Ji, S. D. Chasalow, L. Wang, O. Hamid, H. Schmidt, J. Cogswell, S. Alaparthy, D. Berman, M. Jure-Kunkel, N. O. Siemers, J. R. Jackson, V. Shahabi, An immune-active tumor microenvironment favors clinical response to ipilimumab. *Cancer Immunol. Immunother.* **61**, 1019–1031 (2012). Medline doi:10.1007/s00262-011-1172-6

6. T. F. Gajewski, J. Louahed, V. G. Brichard, Gene signature in melanoma associated with clinical activity: A potential clue to unlock cancer immunotherapy. *Cancer J.* **16**, 399–403 (2010). Medline doi:10.1097/PPO.0b013e3181eacbd8

7. L. V. Hooper, D. R. Littman, A. J. Macpherson, Interactions between the microbiota and the immune system. *Science* **336**, 1268–1273 (2012). Medline doi:10.1126/science.1223490

8. I. I. Ivanov II, K. Honda, Intestinal commensal microbes as immune modulators. *Cell Host Microbe* **12**, 496–508 (2012). Medline doi:10.1016/j.chom.2012.09.009

9. J. P. McAleer, J. K. Kolls, Maintaining poise: Commensal microbiota calibrate interferon responses. *Immunity* **37**, 10–12 (2012). Medline doi:10.1016/j.immuni.2012.07.001

10. N. Iida, A. Dzutsev, C. A. Stewart, L. Smith, N. Bouladoux, R. A. Weingarten, D. A. Molina, R. Salcedo, T. Back, S. Cramer, R. M. Dai, H. Kiu, M. Cardone, S. Naik, A. K. Patri, E. Wang, F. M. Marincola, K. M. Frank, Y. Belkaid, G. Trinchieri, R. S. Goldszmid, Commensal bacteria control cancer response to therapy by modulating the tumor microenvironment. *Science* **342**, 967–970 (2013). Medline doi:10.1126/science.1240527

11. S. Viaud, F. Saccheri, G. Mignot, T. Yamazaki, R. Daillère, D. Hannani, D. P. Enot, C. Pfirschke, C. Engblom, M. J. Pittet, A. Schlitzer, F. Ginhoux, L. Apetoh, E. Chachaty, P. L. Woerther, G. Eberl, M. Bérard, C. Ecobichon, D. Clermont, C. Bizet, V. Gaboriau-Routhiau, N. Cerf-Bensussan, P. Opolon, N. Yessaad, E. Vivier, B. Ryffel, C. O. Elson, J. Doré, G. Kroemer, P. Lepage, I. G. Boneca, F. Ghiringhelli, L. Zitvogel, The intestinal microbiota modulates the anticancer immune effects of cyclophosphamide. *Science* **342**, 971–976 (2013). Medline doi:10.1126/science.1240537

12. I. I. Ivanov II, K. Atarashi, N. Manel, E. L. Brodie, T. Shima, U. Karaoz, D. Wei, K. C. Goldfarb, C. A. Santee, S. V. Lynch, T. Tanoue, A. Imaoka, K. Itoh, K. Takeda, Y. Umesaki, K. Honda, D. R. Littman, Induction of intestinal Th17 cells by segmented filamentous bacteria. *Cell* **139**, 485–498 (2009). Medline doi:10.1016/j.cell.2009.09.033

13. P. López, M. Gueimonde, A. Margolles, A. Suárez, Distinct Bifidobacterium strains drive different immune responses in vitro. *Int. J. Food Microbiol.* **138**, 157–165 (2010). Medline doi:10.1016/j.ijfoodmicro.2009.12.023

14. O. Ménard, M.-J. Butel, V. Gaboriau-Routhiau, A.-J. Waligora-Dupriet, Gnotobiotic mouse immune response induced by *Bifidobacterium* sp. strains isolated from infants. *Appl. Environ. Microbiol.* **74**, 660–666 (2008). Medline doi:10.1128/AEM.01261-07

15. P. Dong, Y. Yang, W. P. Wang, The role of intestinal bifidobacteria on immune system development in young rats. *Early Hum. Dev.* **86**, 51–58 (2010). Medline doi:10.1016/j.earlhumdev.2010.01.002

16. T. Kawahara, T. Takahashi, K. Oishi, H. Tanaka, M. Masuda, S. Takahashi, M. Takano, T. Kawakami, K. Fukushima, H. Kanazawa, T. Suzuki, Consecutive oral administration of *Bifidobacterium longum* MM-2 improves the defense system against influenza virus infection by enhancing natural killer cell activity in a murine model. *Microbiol. Immunol.* **59**, 1–12 (2015). Medline doi:10.1111/1348-0421.12210

17. N. Arpaia, C. Campbell, X. Fan, S. Dikiy, J. van der Veeken, P. deRoos, H. Liu, J. R. Cross, K. Pfeffer, P. J. Coffer, A. Y. Rudensky, Metabolites produced by commensal bacteria promote peripheral regulatory T-cell generation. *Nature* **504**, 451–455 (2013). Medline doi:10.1038/nature12726

18. P. M. Smith, M. R. Howitt, N. Panikov, M. Michaud, C. A. Gallini, M. Bohlooly-Y, J. N. Glickman, W. S. Garrett, The microbial metabolites, short-chain fatty acids, regulate colonic Treg cell homeostasis. *Science* **341**, 569–573 (2013). Medline doi:10.1126/science.1241165

19. K. Atarashi, T. Tanoue, T. Shima, A. Imaoka, T. Kuwahara, Y. Momose, G. Cheng, S. Yamasaki, T. Saito, Y. Ohba, T. Taniguchi, K. Takeda, S. Hori, I. I. Ivanov II, Y. Umesaki, K. Itoh, K. Honda, Induction of colonic regulatory T cells by indigenous *Clostridium* species. *Science* **331**, 337–341 (2011). Medline doi:10.1126/science.1198469

20. M. F. Mackey, J. R. Gunn, C. Maliszewsky, H. Kikutani, R. J. Noelle, R. J. Barth Jr., Dendritic cells require maturation via CD40 to generate protective antitumor immunity. *J. Immunol.* **161**, 2094–2098 (1998). Medline

21. A. Scholer, S. Hugues, A. Boissonnas, L. Fetler, S. Amigorena, Intercellular adhesion molecule-1-dependent stable interactions between T cells and dendritic cells determine

CD8+ T cell memory. *Immunity* **28**, 258–270 (2008). Medline doi:10.1016/j.immuni.2007.12.016

22. S. P. Bak, M. S. Barnkob, A. Bai, E. M. Higham, K. D. Wittrup, J. Chen, Differential requirement for CD70 and CD80/CD86 in dendritic cell-mediated activation of tumor-tolerized CD8 T cells. *J. Immunol.* **189**, 1708–1716 (2012). Medline doi:10.4049/jimmunol.1201271

23. J. Pan, M. Zhang, J. Wang, Q. Wang, D. Xia, W. Sun, L. Zhang, H. Yu, Y. Liu, X. Cao, Interferon-gamma is an autocrine mediator for dendritic cell maturation. *Immunol. Lett.* **94**, 141–151 (2004). Medline doi:10.1016/j.imlet.2004.05.003

24. A. R. Pettit, C. Quinn, K. P. MacDonald, L. L. Cavanagh, G. Thomas, W. Townsend, M. Handel, R. Thomas, Nuclear localization of RelB is associated with effective antigen-presenting cell function. *J. Immunol.* **159**, 3681–3691 (1997). Medline

25. E. B. Compeer, T. W. H. Flinsenberg, S. G. van der Grein, M. Boes, Antigen processing and remodeling of the endosomal pathway: Requirements for antigen cross-presentation. *Front. Immunol.* **3**, 37 (2012). Medline doi:10.3389/fimmu.2012.00037

26. C. Jancic, A. Savina, C. Wasmeier, T. Tolmachova, J. El-Benna, P. M. Dang, S. Pascolo, M. A. Gougerot-Pocidalo, G. Raposo, M. C. Seabra, S. Amigorena, Rab27a regulates phagosomal pH and NADPH oxidase recruitment to dendritic cell phagosomes. *Nat. Cell Biol.* **9**, 367–378 (2007). Medline doi:10.1038/ncb1552

27. C. B. Stober, S. Brode, J. K. White, J. F. Popoff, J. M. Blackwell, Slc11a1, formerly Nramp1, is expressed in dendritic cells and influences major histocompatibility complex class II expression and antigen-presenting cell function. *Infect. Immun.* **75**, 5059–5067 (2007). Medline doi:10.1128/IAI.00153-07

28. K. Kabashima, N. Shiraishi, K. Sugita, T. Mori, A. Onoue, M. Kobayashi, J. Sakabe, R. Yoshiki, H. Tamamura, N. Fujii, K. Inaba, Y. Tokura, CXCL12-CXCR4 engagement is required for migration of cutaneous dendritic cells. *Am. J. Pathol.* **171**, 1249–1257 (2007). Medline doi:10.2353/ajpath.2007.070225

29. M. Nukiwa, S. Andarini, J. Zaini, H. Xin, M. Kanehira, T. Suzuki, T. Fukuhara, H. Mizuguchi, T. Hayakawa, Y. Saijo, T. Nukiwa, T. Kikuchi, Dendritic cells modified to express fractalkine/CX3CL1 in the treatment of preexisting tumors. *Eur. J. Immunol.* **36**, 1019–1027 (2006). Medline doi:10.1002/eji.200535549

30. L. Zhang, J. R. Conejo-Garcia, D. Katsaros, P. A. Gimotty, M. Massobrio, G. Regnani, A. Makrigiannakis, H. Gray, K. Schlienger, M. N. Liebman, S. C. Rubin, G. Coukos, Intratumoral T cells, recurrence, and survival in epithelial ovarian cancer. *N. Engl. J. Med.* **348**, 203–213 (2003). Medline doi:10.1056/NEJMoa020177

31. M. B. Fuertes, A. K. Kacha, J. Kline, S. R. Woo, D. M. Kranz, K. M. Murphy, T. F. Gajewski, Host type I IFN signals are required for antitumor CD8+ T cell responses through CD8alpha+ dendritic cells. *J. Exp. Med.* **208**, 2005–2016 (2011). Medline doi:10.1084/jem.20101159

32. S.-R. Woo, M. B. Fuertes, L. Corrales, S. Spranger, M. J. Furdyna, M. Y. Leung, R. Duggan, Y. Wang, G. N. Barber, K. A. Fitzgerald, M. L. Alegre, T. F. Gajewski, STING-

dependent cytosolic DNA sensing mediates innate immune recognition of immunogenic tumors. *Immunity* **41**, 830–842 (2014). Medline doi:10.1016/j.immuni.2014.10.017

33. C. Blank, I. Brown, A. C. Peterson, M. Spiotto, Y. Iwai, T. Honjo, T. F. Gajewski, PD-L1/B7H-1 inhibits the effector phase of tumor rejection by T cell receptor (TCR) transgenic CD8+ T cells. *Cancer Res.* **64**, 1140–1145 (2004). Medline doi:10.1158/0008-5472.CAN-03-3259

34. J. G. Caporaso, J. Kuczynski, J. Stombaugh, K. Bittinger, F. D. Bushman, E. K. Costello, N. Fierer, A. G. Peña, J. K. Goodrich, J. I. Gordon, G. A. Huttley, S. T. Kelley, D. Knights, J. E. Koenig, R. E. Ley, C. A. Lozupone, D. McDonald, B. D. Muegge, M. Pirrung, J. Reeder, J. R. Sevinsky, P. J. Turnbaugh, W. A. Walters, J. Widmann, T. Yatsunenko, J. Zaneveld, R. Knight, QIIME allows analysis of high-throughput community sequencing data. *Nat. Methods* **7**, 335–336 (2010). Medline doi:10.1038/nmeth.f.303

35. D. McDonald, M. N. Price, J. Goodrich, E. P. Nawrocki, T. Z. DeSantis, A. Probst, G. L. Andersen, R. Knight, P. Hugenholtz, An improved Greengenes taxonomy with explicit ranks for ecological and evolutionary analyses of bacteria and archaea. *ISME J.* **6**, 610–618 (2012). Medline doi:10.1038/ismej.2011.139

36. J. G. Caporaso, K. Bittinger, F. D. Bushman, T. Z. DeSantis, G. L. Andersen, R. Knight, PyNAST: A flexible tool for aligning sequences to a template alignment. *Bioinformatics* **26**, 266–267 (2010). Medline doi:10.1093/bioinformatics/btp636

37. Q. Wang, G. M. Garrity, J. M. Tiedje, J. R. Cole, Naive Bayesian classifier for rapid assignment of rRNA sequences into the new bacterial taxonomy. *Appl. Environ. Microbiol.* **73**, 5261–5267 (2007). Medline doi:10.1128/AEM.00062-07

38. C. Lozupone, R. Knight, UniFrac: A new phylogenetic method for comparing microbial communities. *Appl. Environ. Microbiol.* **71**, 8228–8235 (2005). Medline doi:10.1128/AEM.71.12.8228-8235.2005

39. I. Letunic, P. Bork, Interactive Tree Of Life v2: Online annotation and display of phylogenetic trees made easy. *Nucleic Acids Res.* **39** (suppl.), W475–W478 (2011). Medline doi:10.1093/nar/gkr201

40. M. Barman, D. Unold, K. Shifley, E. Amir, K. Hung, N. Bos, N. Salzman, Enteric salmonellosis disrupts the microbial ecology of the murine gastrointestinal tract. *Infect. Immun.* **76**, 907–915 (2008). Medline doi:10.1128/IAI.01432-07

41. Z. M. Earley, S. Akhtar, S. J. Green, A. Naqib, O. Khan, A. R. Cannon, A. M. Hammer, N. L. Morris, X. Li, J. M. Eberhardt, R. L. Gamelli, R. H. Kennedy, M. A. Choudhry, Burn injury alters the intestinal microbiome and increases gut permeability and bacterial translocation. *PLOS ONE* **10**, e0129996 (2015). 10.1371/journal.pone.0129996 Medline doi:10.1371/journal.pone.0129996

42. J.-P. Furet, O. Firmesse, M. Gourmelon, C. Bridonneau, J. Tap, S. Mondot, J. Doré, G. Corthier, Comparative assessment of human and farm animal faecal microbiota using real-time quantitative PCR. *FEMS Microbiol. Ecol.* **68**, 351–362 (2009). Medline doi:10.1111/j.1574-6941.2009.00671.x